

High level modeling of tonic dopamine mechanisms in striatal neurons

Mark D. Humphries
 Department of Psychology, University of Sheffield
 Sheffield, S10 2TP UK
 m.d.humphries@shef.ac.uk
 Technical Report: ABRG3, November, 2003

Abstract

The extant versions of many basal ganglia models use a ‘gating’ model of dopamine function which enhances input to D1 receptor units and attenuates input to D2 receptor units. There is evidence that this model is unsatisfactory because (a) there are not sufficient dopaminergic synapses to gate all input and (b) dopamine’s main effect is likely to be on the ion-channels contributing to the neuron’s membrane potential. Thus, an alternative output function-based model of dopamine’s effect is proposed which accounts for the dopamine-mediated changes in ion-channel based currents. Simulation results show that the selection and switching properties of the intrinsic and extended models are retained with the new models. The parameter regimes under which this occurs leads us to predict that an L-type Ca^{2+} current is likely to be the major determinant of striatal neuron output if the basal ganglia is indeed an action selection mechanism. In addition, the results provide evidence that increasing dopamine can improve a neuron’s signal-to-noise ratio.

1 Introduction

The action of dopamine at its receptor sites in the striatum has been a source of continuing controversy since it was first established that striatal cells received direct catecholaminergic input from the substantia nigra pars compacta [1]. Primarily the controversy has centered around how dopamine affects striatal output through binding at the two main dopamine receptor sub-types, D1 and D2, expressed by striatal spiny (or projection) neurons.

The prevailing viewpoint is that dopamine acts to attenuate spiny neuron output via D2 receptors and enhance it via D1 receptors and that these receptor types are found on two distinct subpopulations - a view which has informed the dual-pathway models of basal ganglia functional anatomy [2]. To date, all of our computational models of the basal ganglia have also subscribed to this viewpoint [3, 4, 5].

Specifically, we assumed that dopamine acts to gate the input to the striatal spiny neurons, attenuating the input in D2 receptor neurons and enhancing it in D1 receptor neurons. In our previous models, the dopamine level was represented by two parameters: λ_e for the D1 receptor striatal units and λ_g for the D2 receptor striatal units (that is, for the selection and control pathways, respectively — see (author?) [3] for details). The gating effect of dopamine was simulated by using it as a multiplicative factor on the weight vector \mathbf{w} of the afferent connections. Thus, given the afferent input vector \mathbf{c} , the activations at equilibrium \tilde{a}_i^e and \tilde{a}_i^g of the i th striatal D1 and D2 receptor units, respectively, were given by

$$\tilde{a}_i^e = \mathbf{c} \cdot \mathbf{w} (1 + \lambda_e) \quad (1)$$

$$\tilde{a}_i^g = \mathbf{c} \cdot \mathbf{w} (1 - \lambda_g) \quad (2)$$

Using this form of gating assumes that the dopaminergic synapses formed by the substantia nigra pars compacta on spiny neurons are physically positioned after the synapses of other afferent inputs (particularly the glutamatergic input from cortex) and are thus able to affect the synaptic currents generated by these afferent inputs before they reach the soma. However, it is highly unlikely that sufficient dopaminergic synapses exist to meet this assumption: Recent estimates have suggested that as little 4% of spiny neuron dendritic spines receive dopaminergic input, whereas 100% of spines receive at least one excitatory input [6]. Furthermore, dopaminergic input does not elicit a post-synaptic current and so could not electrically gate the input from other afferents.

How then is dopaminergic input to a striatal spiny neuron able to either attenuate or enhance the neuron’s output, depending upon the neuron’s (predominant) receptor type? We leave aside for now the question of

whether the dopamine receptor sub-types do indeed have opposite effects on spiny neurons: it will be seen below that recent studies describing the mechanism of dopamine’s action have also provided strong evidence for this supposition. Our wish is to create a high-level simulation (in keeping with our prior computational models) of dopamine’s affect on the output of spiny neurons via both D1 and D2 receptors and to capture how this effect changes with alterations in dopamine level.

As detailed above, our previous model of dopamine’s action focused on the input to a model neuron. Here we begin by proposing that the effects of dopamine are best captured by directly modeling the affect dopamine ultimately has on the output of the neuron, thereby ignoring the precise locus of its influence — an approach that may be termed *phenomenological* modeling [7]. This approach to modeling dopamine has precedent: a prior simple neural network model emulated the effect of increased dopamine by an increase in the slope of a model unit’s output function [8]. This network was thus able to replicate the finding of increased signal detection performance in a common psychological task (the continuous performance test) following an increase in dopamine level.

Servan-Schreiber et al [8] attributed the dopamine-mediated increase in a neuron’s responsiveness to an increase in the neuron’s signal-to-noise ratio (which would lead to improved discrimination of signal and non-signal events and, in turn, to improved signal detection in the test). By assuming that a neuron’s output $f(x)$ could be modeled as a sigmoid function of its input x

$$f(x) = \frac{1}{1 + e^{-(Gx+B)}} \quad (3)$$

they argued that increasing the slope parameter G (as illustrated in Figure 1) of this function acts to increase that neuron’s signal-to-noise ratio. Further, they showed that any improvement in signal detection performance resulting from the increase requires a minimum circuit of two serially linked units, an input unit for which G may be altered and an output unit which measures signal detection performance (where signal detection was defined as the output of the second unit crossing a threshold).

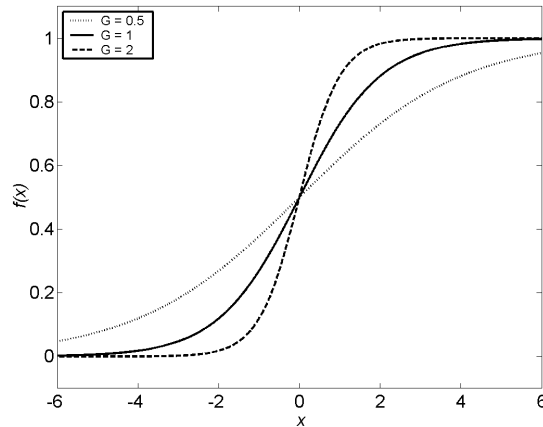


Figure 1: Sigmoid functions relating neuron activation x to normalised output $f(x)$. Increasing the slope parameter G improves responsiveness to excitatory (positive) inputs. Note that the functions pivot about the fixed point $f(x) = 0.5$.

Building on this work, we took as our base assumption that increasing dopamine will alter the slope of a neuron’s output function and extended the model of [8] in two directions. First, their model took no account of the D1 and D2 receptor distinction which crucially underpins our model of basal ganglia function. Therefore, we wished to develop separate output models for striatal spiny neurons with these receptor types. Second, though their connection of psychological results with actual neural output was impressive, we wished to explore a little deeper than the systems level and justify the changes in output function in terms of voltage-dependent ion channels affecting a spiny neuron’s membrane potential (and thus its output). Thus we would

be able to link data from psychology directly to a low-level description of neural mechanisms. Further, it turned out that data on the currents affected by dopamine facilitated our development of separate models for D1 and D2 receptor neurons.

Having developed output models for D1 and D2 receptor neurons, we went on to implement them in both our intrinsic [3] and extended [4] models of basal ganglia function — the extended model embeds the basal ganglia in a thalamo-cortical loop. Simulations of these functional models demonstrated that, with appropriate parameter values, the changes made to the model striatal neurons did not markedly affect either the model basal ganglia’s ability to act as an action selection mechanism or its changes in output following alteration of dopamine level.

2 Methods

2.1 Original neuron output model

The simple leaky-integrator neuron used in our systems-level models had a piece-wise linear output function, that is, a ramp which replicated the strictly increasing portion of a sigmoid function. Thus, the output y of a single neuron given its activation a was given by

$$y = \begin{cases} 0, & \text{if } a < \epsilon; \\ m(a - \epsilon), & \text{if } \epsilon \leq a \leq 1/m + \epsilon \\ 1, & \text{if } a > 1/m + \epsilon \end{cases} \quad (4)$$

where m is the slope of the ramp, and ϵ is a threshold term: giving it a negative value ensures a tonic output from that neuron. In our prior models, striatal units had a threshold of $\epsilon = 0.2$ to simulate the down-state of their biological counterparts. Thus, the minimum activation level of 0.2 required for striatal unit output was taken to be commensurate with the co-ordinated cortical output required to force a spiny neuron into its firing-ready up-state [9]. For simplicity $m = 1$ in all of our published models to date.

2.2 Currents of striatal neurons affected by dopamine

The down-state of a spiny neuron is maintained by an inwardly rectifying potassium current (KIR) which holds the neuron’s membrane potential at approximately -75 mV [10]. There is some evidence from *in vitro* studies that activation of D1 receptors by dopamine or D1-specific dopamine agonists enhances KIR [11, 12] thus driving the neuron’s membrane potential towards the KIR’s reversal potential. In addition, while in the down-state, D1 receptor activation attenuates a depolarising Na^+ current [13]. Therefore, an increase in dopamine level would enhance a D1-type spiny neuron’s down-state and make it less responsive to excitatory input, thereby increasing the level of co-ordinated cortical input required to cause the up-state transition.

Once in the up-state, a spiny neuron’s responsiveness to its inputs is modulated by an L-type Ca^{2+} current, and three outwardly rectifying potassium currents [6]. Dopamine has a direct effect on the L-type Ca^{2+} current via both D1 and D2 receptors [14]. At D1 receptors, dopamine acts to increase the depolarising L-type Ca^{2+} current, thus increasing the neuron’s responsiveness to excitatory input [15]. Conversely, at D2 receptors, dopamine acts to decrease the L-type Ca^{2+} current, thus making the neuron less responsive to excitatory input [16].

The differential effects of D1 and D2 receptors on the L-type Ca^{2+} current would lead to increased and decreased GABA release, respectively, just as reported in rat striatum [17]. Therefore, the long-held assumption that activation of D1 receptors excites and D2 receptors inhibits spiny neurons remains intact. Further, the membrane-potential dependent effects of D1 receptor activation on a striatal neuron’s ion-channels accounts for the oft-cited controversy of whether D1 receptors mediated enhanced [18, 19] or attenuated [20] striatal output.

An intriguing behavioural study of genetically altered mice has provided evidence that the dual effect of D1-receptor activation on striatal output can in turn affect motor activity. Both mutant mice which lack the KIR channel (KIR knockout) and wild-type mice (controls) show significantly elevated locomotor activity following D1 receptor agonist injection [21]. Just such an increase is predicted by our model of basal ganglia function: increased D1 receptor activation would lead to increased striatal output, causing

decreased SNr/GPi output, and thus increased activity via disinhibition of motor-related structures. More pertinently, the KIR-knockout mice had significantly elevated locomotor activity compared to the wild-type mice following the agonist injection. The additional increase of activity in the absence of the KIR channel is consistent with D1's role in simultaneously hyperpolarising spiny neurons via increased KIR while depolarising them via L-type Ca^{2+} currents.

2.3 New neuron output model

Taking the D2 striatal units first, we propose that the attenuation of the depolarising L-type Ca^{2+} current can be captured by a decrease in the slope of the output with increasing dopamine level. Thus, the output y_g of the D2 striatal units is as described by equation (4), except that slope m_g is now expressed as

$$m_g = m_I - \gamma_g \lambda_g, \quad (5)$$

where λ_g is the dopamine level in the control pathway (as before), m_I is the initial value of the slope, and γ_g is a scaling factor. Therefore, increasing dopamine levels correspondingly increases the level of input required to achieve the same output, as illustrated in Figure 2

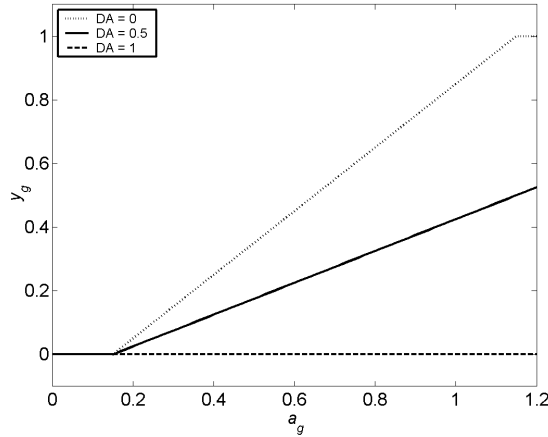


Figure 2: Example outputs slopes for D2 striatal units for $\lambda_g = 0, 0.5, 1$. For these examples, $\epsilon = 0.15$, $m_I = 1$, and $\gamma_g = 1$.

For the D1 striatal units two current effects must be captured, namely the enhancements of both the hyperpolarising KIR and depolarising L-type Ca^{2+} currents following an increase in dopamine level (for simplicity we assume that the attenuation of the Na^+ current is subsumed by the enhancement of the KIR current as both changes have the same end effect). We propose that these antagonistic affects on a neuron's output can be captured by increasing the slope of the output around a fixed pivot point. To do this, we need to both specify an expression for the slope m and rewrite the output expression (4). First, a linear increase in slope m_e with an increase in dopamine

$$m_e = m_I + \gamma_e \lambda_e, \quad (6)$$

where, again, λ_e is the level of dopamine in the selection pathway, γ_e is a scaling factor, and m_I is the initial value of the slope. Second, we add an intercept term to the second output case which sets the pivot point, and thus also have to rewrite its condition

$$y_e = \begin{cases} 0, & \text{if } a < \epsilon; \\ m_e(a - \epsilon) + (1 - m_e)p, & \text{if } \epsilon \leq a \leq (1 - (1 - m_e)p)/m_e + \epsilon \\ 1, & \text{if } a > (1 - (1 - m_e)p)/m_e + \epsilon \end{cases} \quad (7)$$

where p is the desired pivot point of the output, and effectively controls how much each of the KIR and L-type Ca^{2+} channels contribute to the overall output of the unit: setting $p > 0.5$ implies that the KIR has a greater influence; similarly, setting $p < 0.5$ implies that the L-type Ca^{2+} current has a greater influence. Thus, increasing dopamine levels both increases the level of input required to overcome the down-state and decreases the level of input required for the same output (if the down- to up-state transition occurs), as illustrated in Figure 3. As can be seen from Figure 3, ϵ may be more properly called the *initial* threshold

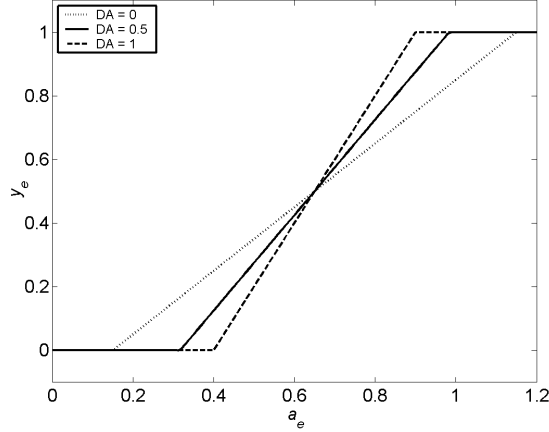


Figure 3: Example outputs slopes for D1 striatal units for $\lambda_e = 0, 0.5, 1$. For these examples, $\epsilon = 0.15$, $m_I = 1$, $\gamma_e = 1$, and $p = 0.5$. The slopes pivot around the output point of 0.5 and thus increasing dopamine increases the amount of activation required to achieve any output while simultaneously increasing the level of output if the activation is sufficiently high. Note that $p = 0.5$ means the KIR and L-type Ca^{2+} currents have an equal magnitude effect on the unit's output.

for the D1 units, as the activation required for any output (and thus the implied threshold) increases with increasing dopamine.

Our proposed D1 unit output function is, with $p = 0.5$, a piece-wise linear approximation of the dopamine model proposed by [8] described above (compare Figures 1 and 3). Based on our simulation results, this will allow us to examine the connection they proposed between improved signal-to-noise ratio and increased dopamine. However, the models were motivated by different underlying premises and thus, whereas their output function necessarily pivoted around $f(x) = 0.5$, our approach is more flexible because it allows for the different effects of the two currents modulated by D1 receptor activation. In addition, we have explicitly created separate output functions for D1 and D2 units in contrast to their general dopamine model.

2.4 Parameters

As a starting point for specifying the parameters for the new output models, we considered what the output of striatal projection neurons would be in the absence of dopamine. Without dopamine there can be no affect on the KIR, Na^+ , or L-type Ca^{2+} currents. Further, there is no reason to believe that the D1 and D2 receptor neurons are otherwise different in any way [22]. Therefore we assumed that for any given input the outputs of D1 and D2 striatal neurons would be identical in the absence of dopamine. In terms of the output models, this implies that both ϵ and m_I should be identical for the D1 and D2 striatal model units so that they have the same output function when $\lambda_e = \lambda_g = 0$. Thus, we set $m_I = 1$ and $\epsilon = 0.1$ for both D1 and D2 striatal units in all the simulations.

In the absence of any contrary data, we assume that the output of D2 receptor spiny neurons does not go to zero following dopamine saturation, and thus we must set $\gamma_g < m_I$ so that there is model D2 unit output at maximum tonic dopamine levels ($\lambda_g = 1$). Thus, we set $\gamma_g = 0.8$ for all the simulations reported here. In addition, we must also assume (in the absence of contrary data) that the magnitude of dopamine's effect is the same for both D1 and D2 receptor neurons, and thus we set $\gamma_e = 0.8$.

No data is available on which of the KIR and L-type Ca^{2+} channels have the greater effect on a striatal neuron’s membrane potential (and, therefore, its output). Thus, we will explore the effects of varying p on the selection and switching capabilities of our intrinsic and extended basal ganglia models so that we may determine which balance of current influence results in optimal behaviour.

Finally, all other parameters (weights, slopes, and so on) were set according to the values given in [23] for the intrinsic model simulations, and those given in [4] for the extended model simulations.

3 Results

As discussed above, we wished to determine how the new dopamine models affected the ability of the basal ganglia to act as a selection and switching mechanism. Therefore, we tested both the intrinsic and extended models with different dopamine and pivot values using a specified set of salience inputs. Dopamine (λ_g, λ_e) and the pivot p were varied over the interval $[0,1]$ in steps of 0.1, giving 121 pairs of dopamine and pivot values to be tested. For each dopamine and pivot value pair, we tested salience inputs c_1 and c_2 over the interval $[0,1]$ in steps of 0.1, that is, for 121 pairs of salience inputs. Thus, both models were simulated a total of 14641 times, once for each dopamine, pivot, and salience input combination. The input to channel 1 began at time $t = 1$, the input to channel 2 began at $t = 2$, and no other channels received input. This gave two time intervals in which basal ganglia output y_i^b on channel i could change: $I_1 = [1 \leq t \leq 2]$ and $I_2 = [t > 2]$. For the intrinsic model, salience was directly input to the striatal units; for the extended model, salience was input to both the motor cortex and striatal units.

Selection of channel i occurred when y_i^b fell below a selection threshold θ_s , which we set at 0.05 in line with our previous work. Using this definition, and given the onset times of the salience input, the outcome of a simulation could be characterised by one of four states:

- First, *no selection*, where $y_1^b, y_2^b > \theta_s$ for all t . Neither active channel becomes selected during the simulation.
- Second, *single channel selection*, where $y_1^b \leq \theta_s$ in I_1 and $y_2^b > \theta_s$ in I_2 ; or $y_1^b > \theta_s$ for all t and $y_2^b \leq \theta_s$ in I_2 . A single channel is selected at some point in the duration of the simulation: either channel 1 becomes selected in the first interval or channel 2 becomes selected in the second interval.
- Third, *simultaneous channel selection*, where $y_1^b, y_2^b \leq \theta_s$ in I_2 . Concurrent channel selection occurs in the second interval (channel 1 must be selected in the first interval to remain selected in the second interval; but note that selection in the first interval does not mean automatic selection in the second interval).
- Fourth, *channel switching*, where $y_1^b \leq \theta_s$ in I_1 and $y_1^b > \theta_s$ in I_2 and $y_2^b \leq \theta_s$ in I_2 . A clean switch between channels: channel 1 is selected in the first interval, then becomes de-selected as channel 2 becomes selected in the second interval.

The outputs of a complete set of salience input pair simulations were summarised by tallying the number of input pairs which resulted in each of the four states. Thus, the question under study can now be broken down into three parts: does implementing the new dopamine mechanism result, first, in sufficient single channel selection and switching for ‘normal’ dopamine levels, second, in realistic changes of the frequency of all four states with changes in dopamine levels and, third, in these two outcomes being achieved using biologically realistic pivot values?

For both the intrinsic and extended models, the answer to all of this is yes. Taking the intrinsic model first, Figure 4 shows that peak channel switching (between 14-19 input pairs) predominantly occurred with moderate dopamine levels of between 0.3 and 0.5 and occurred at low pivot values ($p \leq 0.3$). Single channel selection frequency within these dopamine level and pivot boundaries was also high (63-78 input pairs), though the peak frequency was at $\lambda_e = \lambda_g = 0.2$. Therefore, the results from the new intrinsic model suggest that the effect of the L-type Ca^{2+} current must substantially exceed that of the KIR current for the basal ganglia as a whole to successfully operate as an action selection mechanism.

No selection or switching occurred with no dopamine (Figure 4) as predicted by our model and consistent with the hypothesis that the difficulty of initiating voluntary movement for parkinsonian patients results

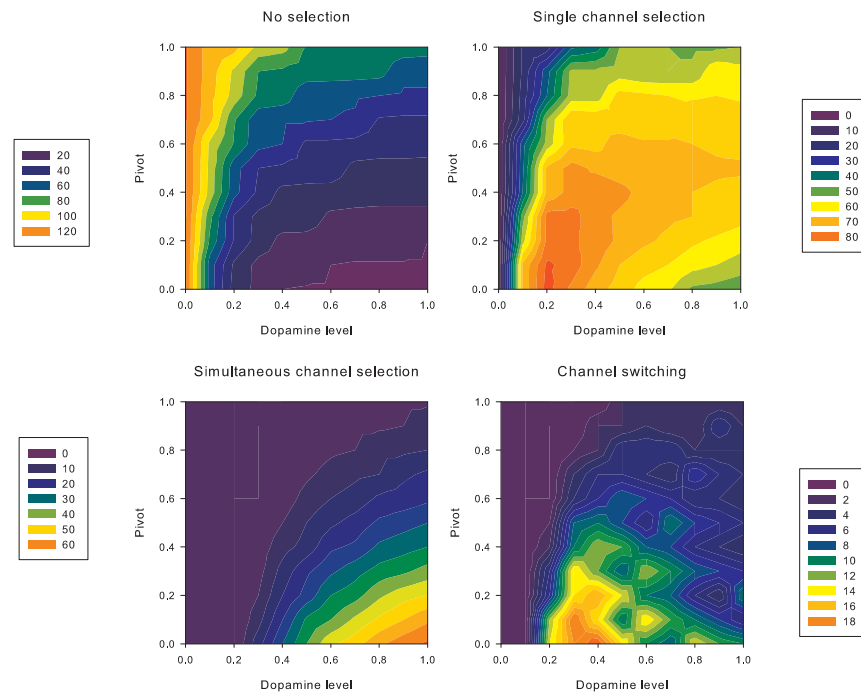


Figure 4: Selection and switching properties of the intrinsic model using the new striatal unit output functions.

from an inability to remove the tonic inhibition by basal ganglia output of motor structures in the thalamus and brainstem. Increasing dopamine to high levels, as might occur following amphetamine stimulation, resulted in a substantial increase in simultaneous channel selection which is indicative of multiply selected or alternated actions. Thus, the model's output following changing dopamine levels does correlate with behavioural problems observed in extreme dopamine conditions. However, again the most accurate outputs were only observed for low pivot values, with simultaneous channel selection only substantially increasing at $p \leq 0.4$.

The extended model results, shown in Figure 5, are surprisingly similar to those of the intrinsic model in that the peak channel switching (25-32 input pairs) occurred with dopamine levels between 0.2 and 0.5, high frequency single channel selection occurred at these dopamine levels, extreme low and high dopamine conditions resulted, respectively, in no selection and high frequency simultaneous channel selection, and all of these results required low pivot values ($p \leq 0.5$). The major difference was that channel switching occurred more often for every dopamine and pivot value pair for the extended model, and that the frequency of channel switching in the extended model exceeded the peak frequency of channel switching in the intrinsic model for 33 parameter pairs, within the pivot range (0.0-0.7) and dopamine values (0.2-0.8). However, beyond $p = 0.5$ there were only two dopamine-and-pivot pairs which showed greater frequency of channel switching than the peak found in the intrinsic model. Thus, in the extended model the basal ganglia's operation as an action selection mechanism was more robust to changes in dopamine and pivot levels. Therefore, the extended model allows for a more flexible hypothesis regarding the balance of the L-type Ca^{2+} and KIR currents in that anything from equal current contributions to exclusively L-type Ca^{2+} current contributions results in sensible selection behaviour.

Having examined the results from the new versions of the intrinsic and extended models, we now need to compare these results with those of the original models to draw firmer conclusions on how the new striatal unit output models have affected the selection and switching properties. To do this we must first identify the parameter set $\{\lambda_e, \lambda_g, p\}$ which resulted in optimal selection and switching performance in the new versions, so that we are able to compare individual simulation sets (that is, a complete set of salience input pairs) across the models. A simple measure of the success of a particular parameter set is the ratio R between the number of input pairs which resulted in successful selection or switching and the number of input pairs which did not (in the simulation set which used those parameters). Expressed formally, this is simply:

$$R = \frac{F_b + F_d}{F_a + F_c}, \quad (8)$$

where F_a , F_b , F_c , and F_d are the frequencies of no selection, selection, simultaneous channel selection, and channel switching, respectively for a simulation set. Thus, the optimal parameter set is that for which R is maximised, constrained by the boundary conditions $0 < p < 1$, because we know that both the KIR and L-type Ca^{2+} channels affect the neuron to some degree, and $0 < \lambda_e, \lambda_g < 1$ because we know that dopamine is not absent from or saturated in striatum under normal conditions.

For the new versions of the models, maximal R occurs at $p = 0.1, \lambda_e = \lambda_g = 0.3$ for the intrinsic model and $p = 0.1, \lambda_e = \lambda_g = 0.2$ for the extended model. Figure 6 shows the comparative frequencies of the four EP output states of the simulation sets corresponding to these parameters and of the original intrinsic and extended models. It can be seen from the histogram that the frequencies of the output states of the original and (optimal) new versions of the intrinsic model are almost identical. Thus, the use of the new striatal unit output functions has not altered the selection and switching properties of the intrinsic model.

The performance of the (optimal) new version of the extended model does differ from the original version. Most striking is that the new version showed no simultaneous channel selection at all, indicating that this particular implementation of the model only ever allows a maximum of one channel to be selected at any given moment - a property which may be termed "hard switching". However, if we consider the parameter set which gives the maximum switching frequency ($p = 0.1, \lambda_e = \lambda_g = 0.3$, the same values as the optimal intrinsic model) then, as Figure 6 shows, the frequencies of the output states of the original and (optimal) new versions of the extended model are again almost identical. Thus, we can conclude that the selection and switching properties of the original extended model *can* be maintained when using the new striatal unit output functions but there is also a different, optimal parameter set which results in hard-switching.

Optimal selection and switching performance was achieved using the lowest possible pivot value ($p = 0.1$) for both the intrinsic and extended models, which implies that, for optimal performance, the influence of

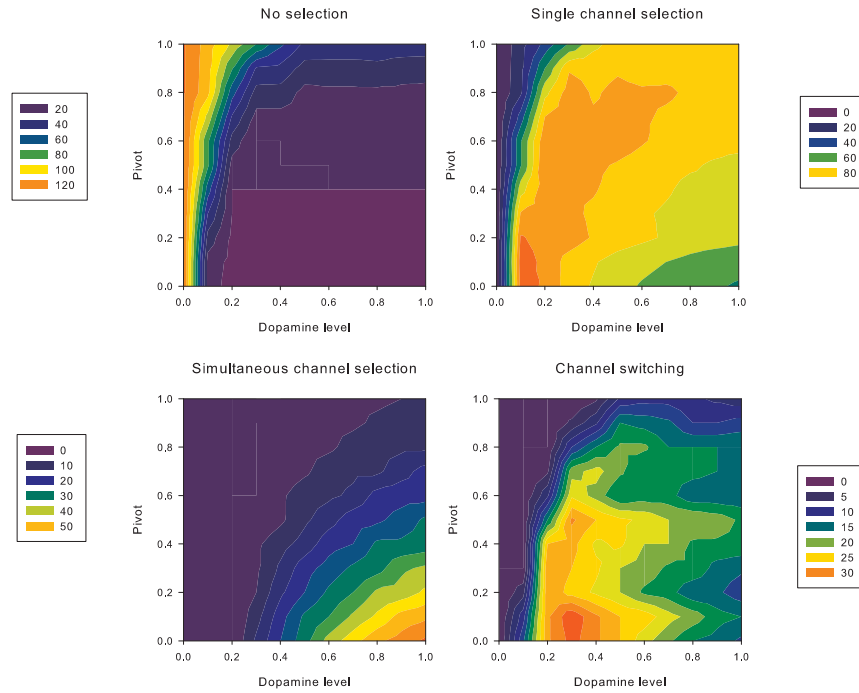


Figure 5: Selection and switching properties of the extended model using the new striatal unit output functions.

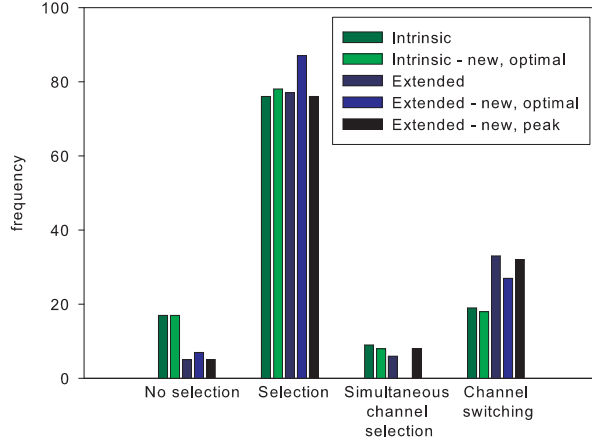


Figure 6: Histogram of the frequency of the four basal ganglia output states resulting from complete simulation sets run on the original and new (optimal) extended and intrinsic models and from the new extended model whose parameter set results in the greatest switching frequency. The frequencies of the output states are almost identical for both versions of the intrinsic model, and for the extended and new peak-switching extended models. Simultaneous channel selection does not occur at all for the new (optimal) extended model, indicating that this model has the property of “hard switching”.

the L-type Ca^{2+} current on the unit’s output must far exceed that of the KIR current. However, as we noted when considering the results of the extended model, near-optimal performance, with high frequencies of switching, can be achieved with a wide range of pivot values.

3.1 Signal detection performance of the new output models

We briefly noted above that the close approximation of our D1 unit output model to Servan-Schreiber et al’s [8] general dopamine model would allow us to examine their claim that increased dopamine improves the signal-to-noise ratio at both cellular and behavioural levels by increasing the slope of a neuron’s output function. More specifically, they demonstrated that by increasing the slope of their (sigmoid) output function, their network model of the continuous performance test was better able to discriminate between signal and non-signal events by virtue of decreasing the number of missed signal events. In addition, they noted that a minimum network of two serial units was required to observe the improvement in signal detection performance.

Translating these findings into our action selection framework, we note direct correspondences with our models: that our signal input is the salience level of the action, that signal detection is indicated by a selected channel, and that our network fulfills the requirement of having the minimum network: an input unit for which the slope is altered (here the striatal D1 and D2 units) and an output unit to observe the signal detection (here the basal ganglia output nuclei). Thus, we predict that increasing the level of dopamine (and thereby altering the slopes of the striatal unit output functions) would lead to increased detection of salient stimuli. This is exactly what we have found: as illustrated in Figure 7 the minimum input value required for single channel selection decreases with increasing dopamine for every pivot value in both the intrinsic and extended models. Thus, increasing dopamine improves both models’ ability to detect signal (salient) events.

It is worth noting that the improved signal detection performance following increased dopamine occurred even though our models utilised two types of striatal units with opposite effects on slope, in contrast to Servan-Schreiber et al’s model [8] which only contained a model roughly equivalent to our D1 model unit. Moreover, the slope of their output function pivoted at 0.5, which in the context of the models presented here would imply an equal influence of the KIR and L-type Ca^{2+} currents on the D1 neuron’s membrane

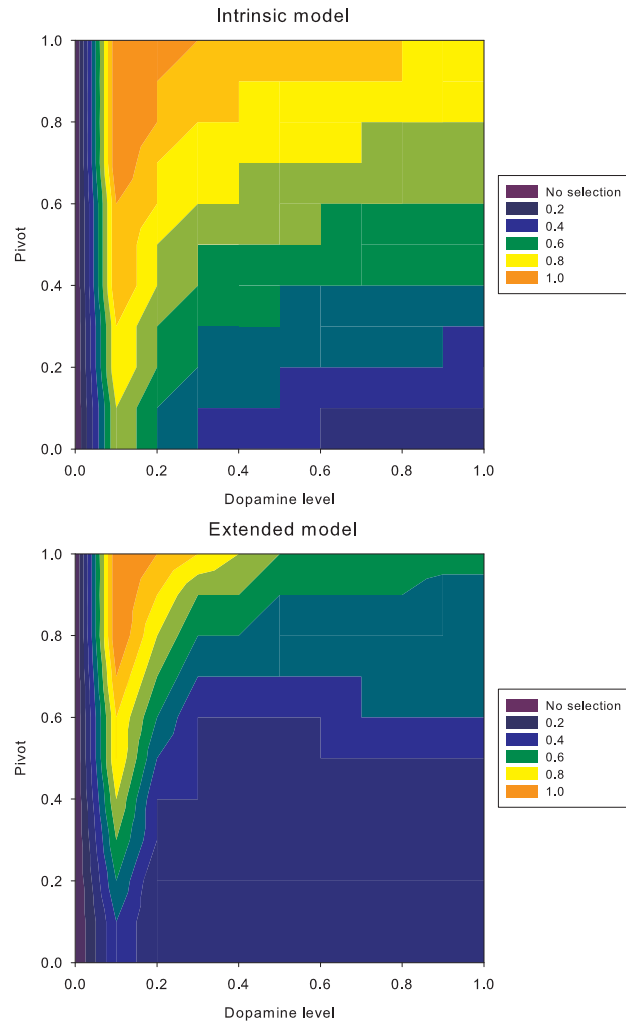


Figure 7: Minimum salience level required for selection of a single channel in the intrinsic (top) and extended (bottom) models.

potential. We have shown that the improvement in signal detection can occur at any pivot point and is, therefore, independent of the exact combination of influences of these two currents. Thus, by using a more accurate model of dopamine’s effects we have been able to provide strong evidence that increasing dopamine will improve signal detection performance.

4 Discussion

We have demonstrated that replacing a gating model with a slope model of dopamine’s effect on striatal unit output has not significantly altered the ability of the simulated basal ganglia to produce outputs consistent with the selection of and switching between salient actions. In addition, the results from the new version of the extended model have suggested that there is an optimal basal ganglia state in which simultaneous channel (and, therefore, action) selection is eliminated, thus only allowing “hard switching” between actions.

The dopamine and D1 output function pivot values for which selection and switching was either replicated (from the original models) or optimal in the new models imply low-to-moderate tonic dopamine and a greater influence of the L-type Ca^{2+} current on the D1 neuron’s membrane potential than the KIR current. Thus, if the basal ganglia is indeed a channel-based switching mechanism in the vertebrate action selection system then we would expect to observe tonic dopamine levels significantly below saturation and greater magnitude effects of the L-type Ca^{2+} than the KIR current in normally healthy, behaving, animals.

Altering D1 output function pivot values did not effect the general trend of decreasing minimum salience input required for selection with increasing dopamine level. If this trend is taken to be indicative of increased signal detection, then we have provided further evidence that increasing dopamine does increase the signal-to-noise ratio of a neuron’s output by altering the neuron’s output function slope, as proposed by [8].

4.1 Assumptions of the slope model

A critical assumption we have made is that the dopamine-modulated ion-channels affecting D1 and D2 receptor neurons give graded response to increases in dopamine, that is, there isn’t a critical level of dopamine at which the channels jump from one state to another, but that their effect continuously varies. An *in vivo* combined voltammetric analysis and single-unit recording study has demonstrated that the strength of both the excitatory and inhibitory responses of striatal medium spiny cells to dopamine release are dependent on the concentration of dopamine (in effect, the tonic level of dopamine) [24]. Thus, we may reasonably expect that as neural output is a continuous function of dopamine level then the currents underlying the generation of this output must also continuously vary in strength.

Other assumptions of the models are open to further testing: we assumed a linear increase in D1 neuron output slope and, correspondingly, linear decrease in D2 neuron output slope with increased dopamine levels purely because this is the simplest possible relationship between slope and dopamine levels. It is certainly possible that either or both of the neuron types have alternate dopamine-slope relationships, such as exponential changes in output slope with increasing dopamine. Further, it is possible that the decrease in output slope of D2 neurons via the attenuation of the L-type Ca^{2+} current is not of equal magnitude to the increase in output slope of D1 neurons via enhancement of the same current, as we have modeled here. Thus, further modeling studies are required to explore the effects of altering the slope’s dopamine-response function and altering the magnitude of dopamine’s effect. (Note also that the linear increase in output slope results in non-linear increase of (implied) output threshold and non-linear decrease of output saturation level for D1 units.)

In addition, the exact slope-dopamine level relationship may be further clarified by *in vitro* or *in vivo* studies. For the D2 neurons, the following is suggested: in slice or culture, voltage-clamped to the up-state (so that L-type Ca^{2+} channel is active) with relatively strong current injection to ensure tonic output of striatal neurons, introduce D2 agonist to extra-cellular bath, and measure (hopefully) decreased output rate of striatal cells with increasing D2 agonist levels. Due to the dual currents active for D1 receptor neurons, a much more complex study would be required, presumably utilising channel-specific toxins to (mostly) eliminate each ion-channel in turn.

There is also the assumption, underlying all of our basal ganglia models to date, of two populations of striatal neurons, divided between D1- and D2-receptor neuron types and their respective projection targets.

Numerous studies have reported that D1 and D2 receptors co-localise on anywhere between 35% and 100% of striatal medium spiny neurons [13, 25, 26, 27]. However, the more recent studies (see, for example, Aizman et al., 2000) have suggested that most researchers (for example, Gerfen et al., 1990) do not find co-localised receptors because D2 receptor concentration is far smaller than D1 in EP/SNr projecting neurons, and D1 concentration far smaller than D2 in GP(e) projecting neurons. Thus, even though they may be co-localised, there is the distinct possibility that their effect (when in minority) is functionally insignificant. However, it would still be prudent to explore the effects of receptor co-localisation in a basal ganglia model, using the new striatal output functions.

4.2 Conclusion

To fully validate the striatal unit output functions presented here, these results require replication at the biophysical level, at which each ion-channel is uniquely described and their spatial effects can be modeled. However, the proposed output functions serve as an interim (and computationally efficient) step with which we have further demonstrated the possibility of capturing complex current dynamics in high-level models and have been able to relate ion-channel effects, neural output, and psychological test data.

References

- [1] L. J. Poirier and T. L. Sourkes, *Brain* **88**, 181 (1965).
- [2] R. L. Albin, A. B. Young, and J. B. Penney, *Trends Neurosci* **12**, 366 (1989).
- [3] K. Gurney, T. J. Prescott, and P. Redgrave, *Biol Cybern* **85**, 401 (2001).
- [4] M. D. Humphries and K. N. Gurney, *Network* **13**, 131 (2002).
- [5] K. N. Gurney, M. Humphries, R. Wood, T. J. Prescott, and P. Redgrave, *Network* **15**, 263 (2004).
- [6] B. D. Bennett and C. J. Wilson, *Synaptology and physiology of neostriatal neurones*, in *Brain dynamics and the striatal complex*, edited by R. Miller and J. Wickens, Harwood Academic Publishers, London, 2000.
- [7] M. D. Humphries and K. N. Gurney, *Neural Netw* **14**, 845 (2001).
- [8] D. Servan-Schreiber, H. Printz, and J. D. Cohen, *Science* **249**, 892 (1990).
- [9] C. J. Wilson and Y. Kawaguchi, *J Neurosci* **16**, 2397 (1996).
- [10] E. S. Nisenbaum and C. J. Wilson, *J Neurosci* **15**, 4449 (1995).
- [11] M. T. Pacheco-Cano, J. Bargas, S. Hernandez-Lopez, D. Tapia, and E. Galarraga, *Exp Brain Res* **110**, 205 (1996).
- [12] D. J. Surmeier and S. T. Kitai, *Prog Brain Res* **99**, 309 (1993).
- [13] D. J. Surmeier et al., *Proc Natl Acad Sci U S A* **89**, 10178 (1992).
- [14] P. Greengard, P. B. Allen, and A. C. Nairn, *Neuron* **23**, 435 (1999).
- [15] S. Hernandez-Lopez, J. Bargas, D. J. Surmeier, A. Reyes, and E. Galarraga, *J Neurosci* **17**, 3334 (1997).
- [16] S. Hernandez-Lopez et al., *J Neurosci* **20**, 8987 (2000).
- [17] W. T. O'Connor, *Nucl Med Biol* **25**, 743 (1998).
- [18] M. Umekiya and L. A. Raymond, *J Neurophysiol* **78**, 1248 (1997).
- [19] F. Gonon, *J Neurosci* **17**, 5972 (1997).

- [20] P. Calabresi, N. Mercuri, P. Stanzione, A. Stefani, and G. Bernardi, *Neuroscience* **20**, 757 (1987).
- [21] Y. A. Blednov et al., *Psychopharmacology* **159**, 370 (2002).
- [22] K. K. Yung and J. P. Bolam, *Synapse* **38**, 413 (2000).
- [23] K. Gurney, T. Prescott, and P. Redgrave, *Biol Cybern* **85**, 411 (2001).
- [24] G. V. Williams and J. Millar, *Neuroscience* **39**, 1 (1990).
- [25] D. J. Surmeier, W. J. Song, and Z. Yan, *J Neurosci* **16**, 6579 (1996).
- [26] J. Harsing, L. G. and M. J. Zigmond, *Neuroscience* **77**, 419 (1997).
- [27] O. Aizman et al., *Nature Neurosci* **3**, 226 (2000).
- [28] C. Gerfen et al., *Science* **250**, 1429 (1990).